J Wood Sci (2005) 51:201–208
DOI 10.1007/s10086-004-0642-2

ORIGINAL ARTICLE

Yoko Midorikawa · Yoji Ishida · Minoru Fujita

Transverse shape analysis of xylem ground tissues by Fourier transform image analysis I: trial for statistical expression of cell arrangements with fluctuation

Received: September 26, 2003 / Accepted: April 23, 2004

Abstract Periodic cell arrangements of tracheids in *Cryptomeria japonica* and *Agathis* sp., and that of wood fibers in *Magnolia obovata* were examined by Fourier transform image analysis (FTIA). The angular distribution functions on power spectral patterns (PSPs) transformed from the dot maps were traced. As well as this conventional method, we developed the line convolution method and domain transformation for more correct analysis of radial and tangential arrangements. Cell arrangements became clear in *Cryptomeria* and *Agathis*. Fluctuations were expressed by the standard deviation (σ) or the relative standard deviation (σ_r) so that we could compare the characteristics of both woods. In *Cryptomeria*, the most provable distance between tracheids along radial files was 36.7 μm with 17% fluctuation, whereas the tangential interval was 28.3 μm with σ_r of 24%. In *Agathis*, the radial diameter was 35.1 μm with σ_r of 23% and the tangential interval was 41.5 μm with σ_r of 23%. In *Magnolia*, the maximal periodicity of wood fibers was 15.8 μm and 20.5 μm along and between radial files, respectively, although the fluctuations could not be estimated because of the remarkable interruptions by numerous vessels.

Key words Tracheid arrangement · Fiber arrangement · Periodicity · Cell arrangement fluctuation · Fourier transform

Introduction

Wood is an assembly of cells. When regarding xylem ground tissues, tracheids, and wood fibers as "structure elements," the wood structure on the transverse section can be understood in terms of three kinds of "shape factors," namely, cell arrangements, cell shapes, and cell wall thickness.[1] Because the shape and arrangement are closely related, actual wood characteristics will become clear by analyzing the cell assembly pattern in addition to each cell property. We examine cell arrangement in this report, and cell shape in the following report. Cell wall thickness was also analyzed.[2,3] If the analysis is limited to only the structural characteristics of each cell, the usual ordinary accumulation image analysis (OAIA) is sufficient. On the other hand, Fujita et al.[4–6] and Hata et al.[7] analyzed the group of cells as a periodic structure rather than each individual cell and they introduced a new technique to analyze the cell group using the two-dimensional Fourier transform method. The dot map (DM) method was developed, which placed a uniform point in the center of each cell on the transverse section to clarify the cell arrangement.[4,6] The most frequent (abundant) cell arrangement in the two-dimensional analysis was measured from the characteristic of the power spectrum pattern (PSP) which was output by fast Fourier transform (FFT)-processing of the DM. It was by analysis of PSP of the DM (DM-PSP) that the oblique arrangement of tracheids in softwood was detected for the first time[4] and new properties of vessel distribution were shown to be different from observations made with the traditional microscope.[8] More precise analysis of the power distribution demanded comparison of many specimens. Maekawa et al.[9] and Fujita et al.[10] developed a program for PSP polar coordinate analysis and demonstrated the tracheid and wood fiber cell arrangement by analyzing the power concentration, namely, the relative height of power. By surveying the appearance of peaks and their heights that reflect the cell arrangements, comparison among specimens became possible. However, examination of the diffusion of the peak was not performed.

Before using FFT, pictures need to be transformed into discrete data. There are various equipment problems, including narrowness of the power brightness range. In a previous report, we examined the occurrence of errors due to picture sampling and the discrete images[1] and problems

Y. Midorikawa · M. Fujita (✉)
Division of Forest and Biomaterials Science, Graduate School of Agriculture, Kyoto University, Kitashirakawa-Oiwake-cho, Sakyo-ku, Kyoto 606-8502, Japan
Tel. +81-75-753-6238; Fax +81-75-753-6302
e-mail: kzfujita@kais.kyoto-u.ac.jp

Y. Ishida
Wajima General Agriculture and Forestry Office, Ishikawa 928-8525, Japan

Table 1. Definitions of abbreviations and notations

Abbreviation or descriptor	Definition or explanation
OAIA	Ordinary accumulation image analysis
FTIA	Fourier transform image analysis
Structure elements	Objects such as tracheids or vessels
Shape factor	Shape such as diameter or area of structural elements.
Pre-FFT	Procedures on the image domain, such as extraction of structure elements and shape factors, and also convolution to enhance the power level
Post-FFT	Procedures on the frequency domain such as the polar coordinate analysis
Assembled tissue	Xylem tissue assembled with uniform size and shape of cells, such as tracheids in softwood
Dispersed tissue	Xylem cells such as vessels dispersed in the ground tissue
$P(\phi)$	Angular distribution function of PSP
$P(k)$	Frequency distribution function of PSP
sNM	Selective net map which consist of only objective structure element, such as a body-NM and a tip-NM made from contours of only the cell body part or cell tip, respectively
E_{SPN}	Shortage error of periodic number
$P_{eq}(k)$ and $P_{mer}(k)$	Frequency distribution functions of PSP along the equator and the meridian
Period (τ)	Periodicity distribution function
Max-o	Original maximum; the most frequent period directly calculated from the original frequency distribution function
Max-s	Peak-separated maximum; the most frequent period after the peak separation of the periodicity distribution function, equal to τ_{max}
ϕ_{max}	The angle that has maximum value of $P(\phi)$
k_{max}	The frequency pixel that has maximum value of $P(k)$ except 0 (the origin)
τ_{max}	The period that has maximum value of main peak of peak-separated *Period* (τ)
σ_r	Relative standard deviation
DcDM	Disc-convoluted dot map
LcDM	Line-convoluted dot map

associated with Fourier transform image analysis (FTIA).[11] It became clear that the concept of convolution on the images and the Radon transformation, and the δ function, normally considered an error, could be used to our advantage.[11] Therefore, we analyzed "fluctuation," which is not clearly defined, in addition to the most frequent periodicity. Because wood is a natural product, the arrangement of cells exists between periodicity and randomness. Then, for the present, considering the disorder from the complete periodicity as fluctuation, we evaluated the fluctuation by use of the power diffusion on PSPs.

The terms and abbreviations associated with OAIA and FTIA were announced in previous reports[1,3,11] and parts of them are shown here. Table 1 shows a list of abbreviations used throughout this report.

Materials and methods

Specimens and microscopic preparations

For verification of the results, we selected uniform samples, namely, the early wood of *Cryptomeria* representing little change in cell arrangement and shape, and *Agathis*, a tropical softwood with a relatively constant structure and no annual rings. On the other hand, *Magnolia* was chosen as an example of hardwood fiber, because its cell arrangement was the most disperse among many Japanese hardwoods tested by Maekawa et al.[9] and Fujita et al.[10] The microscopic preparations were described previously.[1,11] The process involved treatment of the wood block with 55% HF, epoxy resin embedding, slicing of 5-μm-thick transverse sections, safranine staining, and balsam mounting.

Original picture sampling and equipment

When quantitatively analyzing the range of fluctuation, it is necessary to obtain a large number of structure elements. We used very low-magnification photographic conditions of 2× (objective lens) and 2.5× (projection lens) for *Cryptomeria* and *Agathis*, and 4× and 2.5× for *Magnolia*, to sample as many cells as possible at a time. The photographic pictures were transformed to digital images by a high-resolution film scanner at 1280 dpi.[1,12] The limitation factor of the resolutions was R_D (4.0 μm in *Cryptomeria* and *Agathis*, and 2.0 μm in *Magnolia*). We selected Luzex III (Nireco) as the main image processor, because it expresses the Perceval equation without suppression of power brightness.[11] The input method of the transverse section image was the same as previously reported. For example, the direction of radial growth was adjusted to coincide with the x-axis on the display screen.[1,11,12]

Extractions of structure element and shape factor, and some operations

We made input pictures into discrete images, namely, cell wall maps (WM) or cell lumen maps (LM). In *Cryptomeria* and *Agathis*, a small number of ray parenchyma cells was involved, although almost all cell lumens were those of tracheids. Because ray lumens were so slender along the

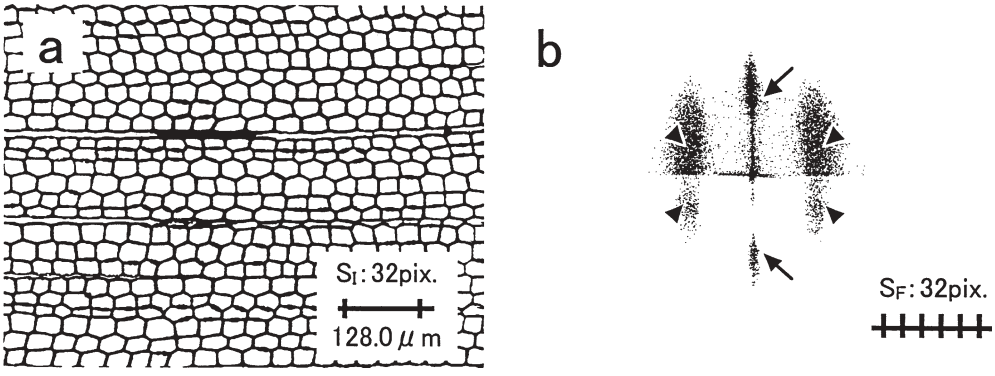

Fig. 1a,b. Result of Fourier transform image analysis (FTIA) procedure on a cross sectional view of *Cryptomeria japonica.* **a** A part of the discrete image of the original picture input to the image analyzer. **b** Discrete image of dot map-power spectrum pattern (DM-PSP), showing the power along the meridian on which spots can be recognized (*arrows*). Four spots (*arrowheads*) are located on the two striations and suggest a honeycomb assembly of tracheids. The lower half was output at lower brightness than for the upper half

x-axis, they were excluded by size filters. Axial parenchyma cells were ignored. The example of *Cryptomeria* is shown in this article (Fig. 1), while those of *Agathis*, shown in previous reports[1,11] are omitted here. In *Magnolia*, lumens were extracted and those of vessels and rays were deleted to give only wood fibers.

For extraction of the shape factor, each lumen was simplified to the central point of cells that constituted one pixel, namely, the dot map (DM) according to the method proposed by Maekawa et al.,[9] and it was cut off in a circular window.[11] To reinforce power, dots were expanded uniformly using the method of Maekawa et al.[9] This map and the PSP are called the disc-convoluted dot map: DM, DM-PSP, respectively. We used the polar coordinate analysis program developed by Maekawa et al.[9] and Fujita et al.[10] for analysis of PSP. In addition, we developed a new convolution and analysis system as follows.

Results and discussion

Power reinforcement and concentration effects by line convolution

Dot maps with a large fluctuation in their arrangement resulted in only a weak power level, even if there were more than 1000 dots. Until now, the DM method has been used for power reinforcement with pre-FFT (see Table 1). An example for *Cryptomeria* is shown in Fig. 1. This method is convenient for visual judgment of the PSP because the PSP is output onto an Airy disc preserving the two-dimensional information. However, the power decreases with the frequency pixels (k) and it generates the so-called missing order of an Airy disc around 250,[11] so quantitative analysis of a frequency distribution function will be limited to the low frequency domain. Although Maekawa et al.[9] performed a "deconvolution operation" using a random dot map PSP for the offset of this weak point, this method was very complex. Therefore, we developed a very simple and effective technique based on the principle of the Radon transformation. In the example shown in Fig. 2, each dot was extended up and down for four pixels (nine pixel lengths in total) and the power was amplified nine times by convolution. The operation by which dots are extended vertically or horizontally is very easy for the image processor. Also, another effect can be added on the power distribution that is spread into the two dimensions in case of DcDM-PSP. That is PSP of line convoluted dot maps (LcDMs) is concentrated and amplified near the equator line by 1024/9 (Fig. 2b). As these extended lines are one pixel in width, periodic information is maintained in the x-direction by the Radon transform effect. That is, each extended line has a strong point as the δ function as described in the previous report.[11] This convolution method was so useful that LcDM-PSPs were used to examine the fluctuation of arrangement in radial and tangential directions.

On the other hand, we contrived another technique to extract only the wood fiber bodies and enhance the power (Fig. 3). In the usual net map (NM), the cell boundary is extracted. In softwoods, each neighboring tracheid shares this boundary line. However, when adjacent cells are of different types, the cell boundary line must be made clear. There are many vessels and ray parenchyma cells in hardwoods. Moreover, there is a difference between the body part and the tip part. Therefore, we developed the technique described below to determine the origin of body parts. At first, the NM was expanded to five pixels wide (this width can be optionally selected according to software of the equipment) and the reverse image was made. Size filters removed vessels and rays, and then the body part (Fig. 3b) of large size was divided from the small tip part with triangle or diamond form by a size filter. The ratio of the tip part to the body part was about 0.3. When these lumens are processed to dots, the selective dot maps are called "body-DM" and "tip-DM," respectively. On the contrary, the differential filter can extract the edge of lumens, although the positions are shifted from the true wall–lumen boundaries. The main purpose of this pre-FFT processing is cell shape analysis, but the reinforcement effect of the power was remark-

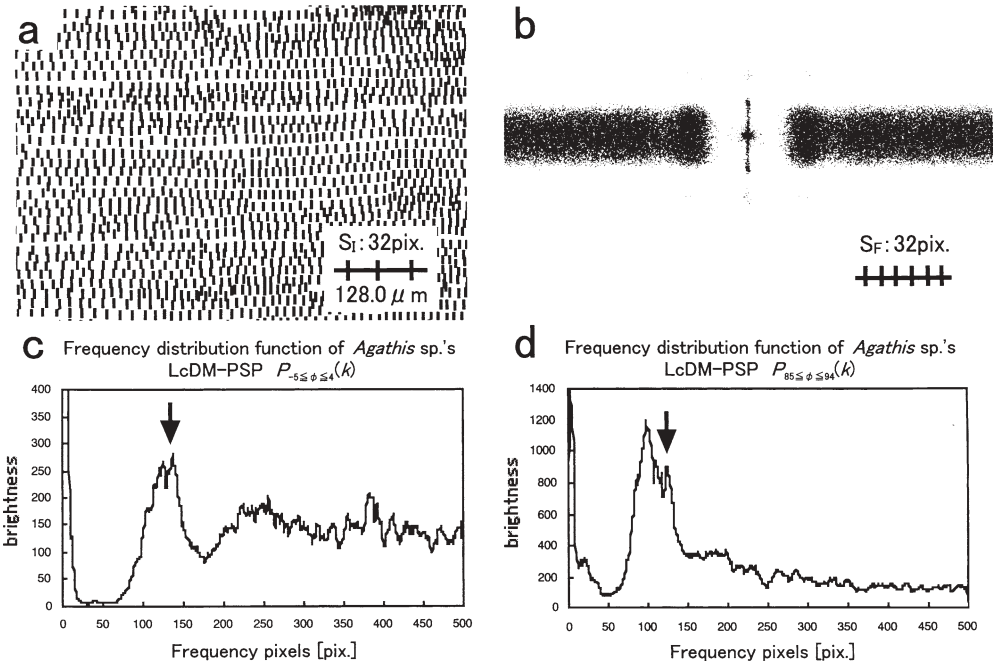

Fig. 2a–d. Line convolution effect in *Agathis* sp. **a** Line convoluted dot map (LcDM) consisted of dots elongated vertically to nine pixels. Lines are dilated by two pixels in the horizontal direction for clarity. **b** LcDM-PSP. **c** Frequency distribution function on the equator of LcDM-PSP [$P_{eq}(k) = P_{-5\leqq\phi\leqq4}(k)$]. **d** Frequency distribution function on the meridian of LcDM-PSP [$P_{mer}(k) = P_{85\leqq\phi\leqq94}(k)$]. Note LcDM-PSP in **b** shows that the power is concentrated around the equator. Although large peaks are clear in **c** and **d**, additional peaks are also detected slightly (*arrows*)

able. This is called a "body-NM," which is one of the selective NM (sNM). The power is expressed around $k = 200$ corresponding to paired boundaries.

Visual analysis of DcDM-PSP

Interpretation of PSPs that are presented on the two-dimensional polar coordinates of the frequency domain needs practice because phase information on their original image domain was erased. Moreover, size information is expressed by a reciprocal.[11] However, when an input picture is simplified to DcDM by pre-FFT, the visual understanding of PSP is not difficult (Fig. 1). Tracheids and wood fibers produced from the fusiform initials by the periclinal division make a series of cells, that is, radial file. The arrangements of intraradial files appear on the equator line of DM-PSP, whereas those of interradial files are expressed on the meridian.[11]

In *Cryptomeria*, two types of striations were observed; one was the meridian striation, the other was a paired striation at frequency pixel $k = 118$ stretched in parallel to the former (Fig. 1b). There were two concentrated parts of power at $k = 150$ on the meridian striation (arrows in Fig. 1b). The power spots were also detected at two points on paired ones (arrowheads in), respectively, then six centering parts in the amount existed. This result was the same in *Agathis*.[11] It suggested that tracheids were put together like a honeycomb ambiguously, but the arrangement surely existed.[4–6]

In case of *Magnolia*, the power having a ring was observed as in an analysis example in a previous report by Maekawa et al.[9] However, when observing in detail, striations that stretched along the direction of the meridian were observed. Figure 3d shows DcDM-PSP that was generated from the body-DM (Fig. 3c) and in this PSP the striation is clearly observed (arrows). On the other hand, the same characteristics were also observed in the tip part PSP (PSP was omitted). These facts suggest that the body part and tip part together were arranged in the radial direction. No other peculiar power was discovered from the tip part PSP. The power concentrations were also observed in the oblique direction, in which arrowheads pointed in the body part PSP shown in Fig. 3d. However, the power was so diffuse that specifying a maximal part was not easy. Because the power was weak in DcDM-PSP, we examined it more in the sNM-PSP (Fig. 3f) generated by the FFT process from the sNM, namely, the body-NM shown in Fig. 3e. A power distribution similar to the case of DcDM-PSP was observed in the low-frequency domain (arrowheads) and moreover the power like a ring appeared at about $k = 200$ in the middle-frequency domain. Other spots in the equator direction were detected in addition to the spots on the meridian and the oblique direction. Eight spots could be specified (arrows) due to the effect that boundary lines composed of two lines with a five-pixel interval reinforced and concentrated the power in a ring as described.

Reconstruction of the most frequent model of tracheid and wood fiber arrangements

Tracheids and wood fibers produced from the fusiform initials by the periclinal division make a radial file. The cell arrangement of the intraradial file appears on the equator of the DM-PSP. For more precise quantitative analysis and the concrete reconstruction of cell arrangements, we obtained the frequency distribution function $P(k, \phi)$ of LcDM-PSPs from the sector $-5 \leqq \phi \leqq 4$ including the equator, and $85 \leqq \phi \leqq 94$ including the meridian (Fig. 2c,d).

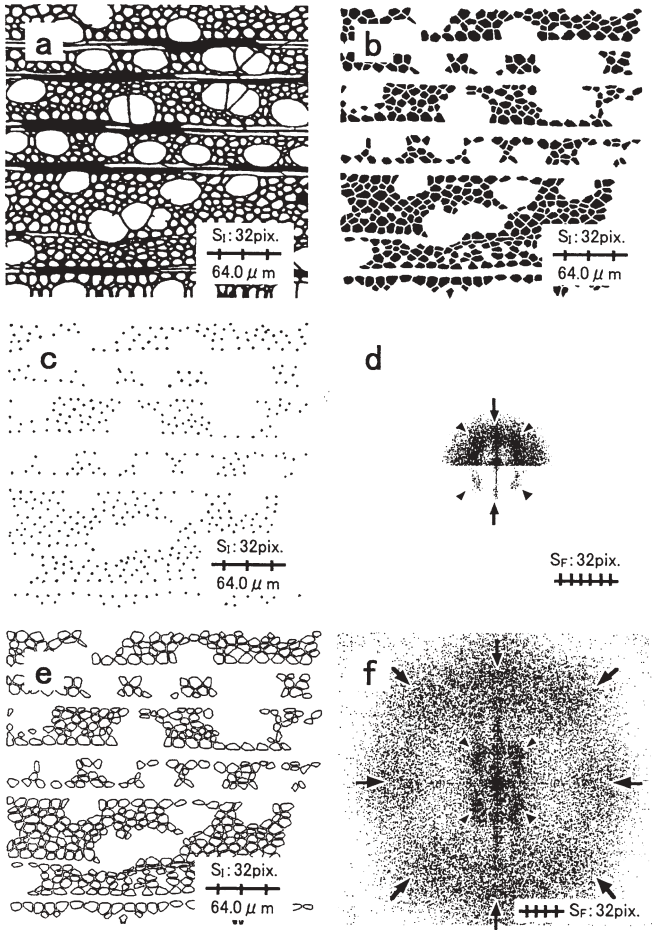

Fig. 3a–f. The general procedure of FTIA to extract only the body part of wood fibers in *Magnolia obovata*. **a** Part of discrete image of original picture. **b** Lumen map of body part extracted after the removal of fiber tips, vessels, and rays by size filters. **c** Disc convoluted dot map (DcDM) from **b**. **d** DcDM-PSP. **e** Selective net map (sNM), especially called a body-NM, produced by differentiation of lumens in **b**. **f** sNM-PSP. DcDM-PSP shows that the power is distributed circularly and some spots are discerned on the circle (*arrows* and *arrowheads*). A lower half was outputted at lower brightness than for the upper half in **d**. sNM-PSP shows similar spots (*arrowheads*) to **d** and further spots on a higher frequency power ring (*arrows*)

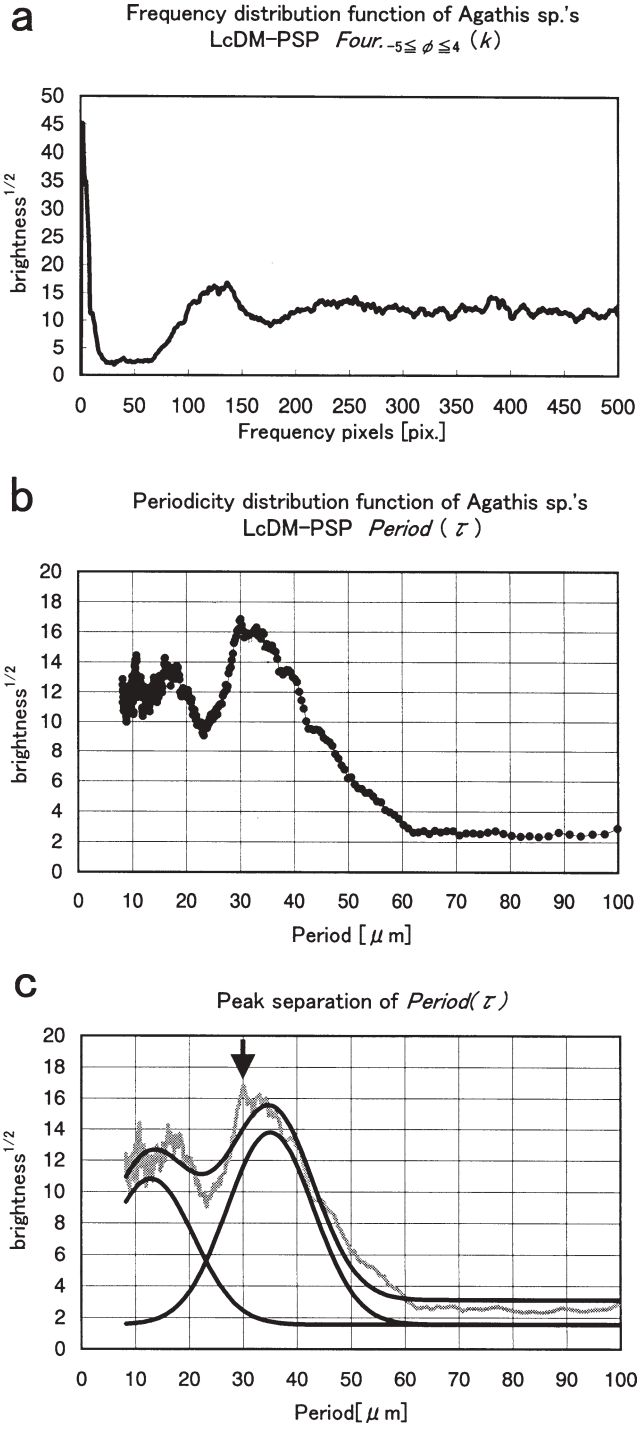

Fig. 4a–c. Periodicity analysis in r-direction in *Agathis* sp. **a** Fourier spectrum calculated from the frequency distribution function on the equator of LcDM-PSP (Fig. 2c). **b** Periodicity distribution function on the horizontal axis transformed from **a**. **c** Peak separation of **b** by using the Sigma Plot software package. Note that although the periodicity distribution function was well separated, further peaks remain (*arrow*)

As described in a previous report,[11] we designated the brightness distribution function of the map as $B(x, y)$, the Fourier spectrum as $Four.(k, \phi)$, and the power spectrum as $P(k, \phi)$. Here, we propose the periodicity distribution function $Period(\tau, \phi)$ of the map. Because discussion is often focused on a certain direction, we express $Four.(k, \phi)$, $P(k, \phi)$, and $Period(\tau, \phi)$ as $Four.(k)$, $P(k)$, and $Period(\tau)$, respectively. Analysis starts from $P(k)$ (Fig. 2c). $P(k)$ was changed to $Four.(k)$ by calculating the square root of the vertical axis (Fig. 4a), and changed to $Period(\tau)$, which was obtained by translating the horizontal axis reciprocally (Fig. 4b), namely, $\tau[\mu m] = 1024/k$ [pixels] $\times$ 4.0 [μm/pixel]. $Period(\tau)$ was submitted to the peak separation software Sigma Plot to obtain the maximum τ (τ_{max}). Separation assumptions and factors are as follows: a function curve is separated as a normal distribution function and a curve consists of a main (primary) peak and a sub (high-order) peak. Peak height (a); $a_{main} > a_{sub}$, peak position (x); $x_{main} > x_{sub}$, constant value (c); $c_{main} = c_{sub}$. The correlation coefficient R was examined, $R = 0.945$ (Fig. 4c). Finally, from the τ_{max} cell position was calculated in the radial and tangential directions. In Table 2, Max-s (peak-separation

Table 2. Values on tracheid and fiber arrangements calculated from the angular and frequency distribution functions of DM-PSP

Samples	Power spectral pattern		Calculated periodicities		
	ϕ_{max}[b](degrees)	k_{max}[c](pixels)	Max-s[d] ± σ(μm)	σ_r[e](%)	Max-o[f](μm)
Cryptomeria japonica	0 (r-direction)	118	36.7 ± 6.1	17	34.7
n[a] = 6000	90 (t-direction)	150	28.3 ± 6.9	24	27.3
	156 (oblique direction)	127	–	–	32.3
Agathis sp.	0 (r-direction)	123	35.1 ± 8.0	23	33.3
n = 6600	90 (t-direction)	98	41.5 ± 9.5	23	41.8
	159 (oblique direction)	130	–	–	31.5
Magnolia obovata	0 (r-direction)	130	–	–	15.8
n = 3100	90 (t-direction)	100	–	–	20.5
	46 (oblique direction)	86	–	–	23.8

[a] Number of structure elements
[b] The angle that has maximum value of angular distribution function
[c] The frequency pixel that has maximum value of frequency distribution function except 0 (the origin)
[d] The most frequent period after the peak separation of the periodicity distribution function, equal to τ_{max}. The curve was separated as a normal distribution and σ was calculated mathematically
[e] Relative standard deviation (100 σ/Max-s)
[f] The most frequent period directly calculated from the original frequency distribution function

maximum) denotes τ_{max}. A concentration of power in the oblique direction was detected in both softwoods and hardwoods.[9,10,13] This indicated that the cell was arranged in the oblique direction, and we measured the maximum angle (ϕ_{max}) from the angular distribution function P (ϕ) of DcDM-PSPs (Table 2).

In the same procedures conducted with *Magnolia*, k_{max}, which is the frequency pixel that has maximum value of P (k), was obtained from the body-LcDM-PSP (Table 2). However, the peaks on both the equator and the meridian were different those for softwood. They were prominent on only one part of them (graphs not shown). k_{max} in Table 2 shows this prominent part and Max-o (original maximum) is the period that is directly calculated from k_{max} of the PSP by a conventional technique. The arrangement of the oblique direction was obtained from ϕ_{max}, which was weak but was detected in $P(\phi)$ of DcDM-PSP. Although this angle could not be detected in the visual judgment of DcDM-PSP (Fig. 3d), concentrated powers in the oblique direction could be distinguished in the visual judgment of sNM-PSP (arrowheads in Fig. 3f). The angles of these powers were almost the same as ϕ_{max} of DcDM-PSP.

A model of cell arrangement with the highest possibility was reconstructed from the information in Table 2 and is shown in Fig. 5. A model restored by the central point of cells is called a dot model. However, the dot model is a very different image from that of the actual transverse section, which prompted us to prepare the block model. In softwood, tracheids were considered an assembled tissue, because cell walls were situated on the middle of the dots, and a line was used to divide each dot at the center (Fig. 5a,b). Cell wall angles cannot be determined until angle analysis is done (this will appear in the following report). Tracheid shape was supposed to be rectangular considering the radial files. This model is called a block model because it resembles a brick wall. Seeing block models of *Cryptomeria* and *Agathis*, they are rectangular. When the comparison is made between sideways and longways, the former is longer sideways and the latter is shorter sideways, respectively. Thus, characteristics among species can be clarified. On the other hand, the dot model of *Magnolia* was reconstructed only with the body part of wood fiber, because the tip part was removed. Therefore, a block model was not reconstructed in this step.

Experimental conditions for fluctuation analysis

Dot models and block models were restored from the maximal part of the power on DcDM-PSP, LcDM-PSP, and so on. These models are thought to represent the most frequent cell arrangements extracted from the whole sampling area. However, actual PSPs show high diffusion, being different from the case of X-ray diffraction of crystals. This means that actual cell arrangements in woods are not uniform. They have considerable "fluctuation" as is usual with natural products. We are sure the fluctuation is related to the species and age of trees, and also affects wood properties. Maekawa et al.[9] obtained the angular distribution function and the frequency distribution functions in 17 species and then obtained the relative peak heights to whole power using the deconvolution and normalization method. This was followed by work by Fujita et al.,[10] and Diao et al.[13] covering many specimens. This method is effective for comparison between specimens but does not really relate to the essence of fluctuation. Also, most of peaks were in the low-frequency bandwidth; the concern over frequency errors R_F[11] is large. Considering these points, we set the environment to control the occurrence of various errors to within 10% as previously reported.[1,11] Analysis conditions were chosen to minimize the frequency error (E_F), considering the optical resolutions (R_O) and discrete resolution (R_D).[1,11,12] Enormously abundant cells can make fine scanning possible to determine frequency distributions. Each cell was sampled at the size of about 10 pixels at low magnification and the negative influence of R_F was avoided.[11]

Next, we examined diffusion of peak caused by "shortage of periodic number" (spn). When there are few

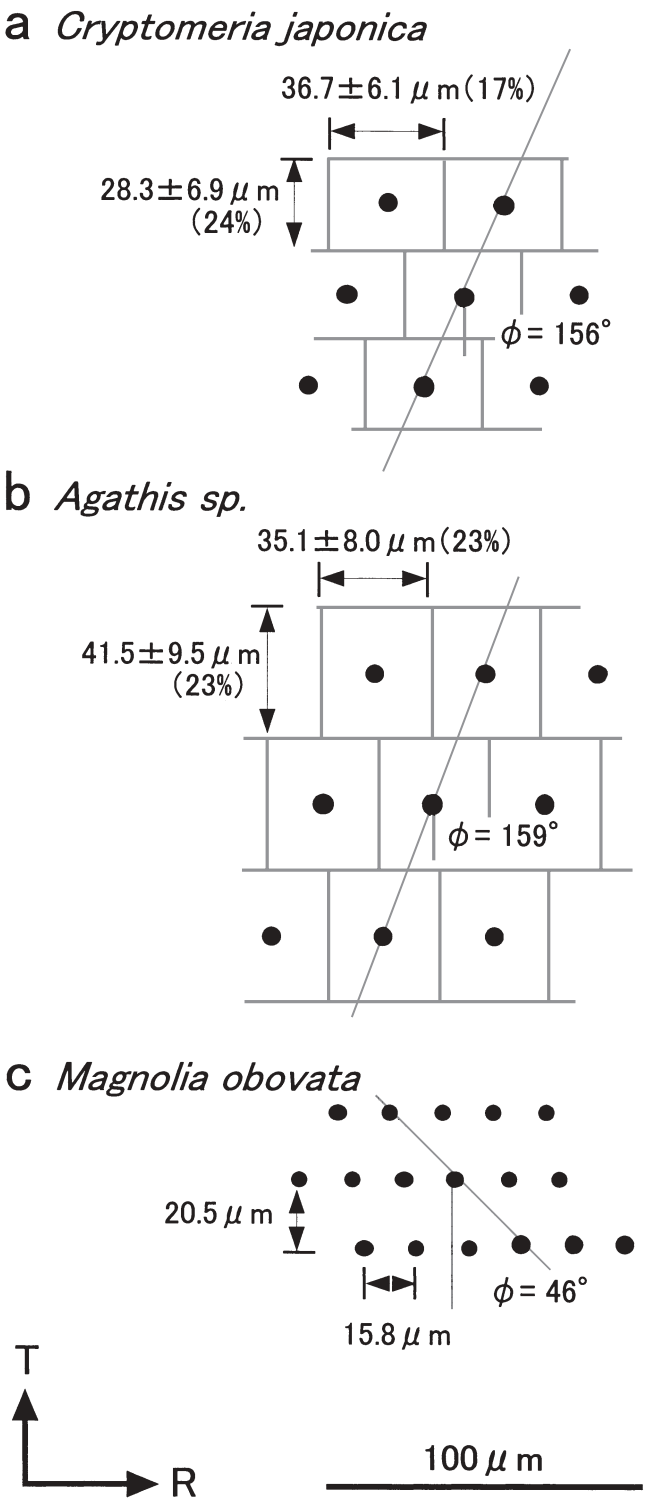

Fig. 5a–c. Reconstruction of cell arrangements and fluctuations. **a** Dot model and block model of *Cryptomeria japonica*. **b** Models of *Agathis* sp. **c** Dot model of *Magnolia obovata*. The most abundant period, the standard deviation, the relative standard deviation, and oblique arrangement (ϕ) were added to models. Values are selected from max-s in *Cryptomeria japonica* and *Agathis* sp. and max-o in *Magnolia obovata* (see Table 2)

numbers of periods even if the period is not disordered, power will inevitably diffuse due to the uncertainty principle.[14] The Scherrer formula of the X-ray diffraction is based on this effect, and, conversely, crystal width can be calculated from the diffusion of peaks. Periodic number depends on specimen characteristics, for example, in hardwood, vessels interrupt fiber rows. We designated the error of spn (E_{SPN}) as a ratio of brightness value in the pixel next to the frequency pixel that had the maximal brightness value. E_{SPN} was ignored when the period number was 50 or more and E_{SPN} became less than 10% by use of a vertical line pattern as in a previous report.[11] Because the cell number of this examination was about 6000 in *Cryptomeria* and *Agathis* and about 3000 in *Magnolia* (Table 2), i.e., about 80 and 55, respectively, in one dimension, it was thought that power diffusion of the PSP reflected the fluctuation between each dot's distance, not the spn error.

Detection of fluctuations in three species and conclusions

Power diffusion on LcDM-PSP of *Agathis*, for instance, at $P_{-5\leqq\phi\leqq4}(k)$, namely, $P_{eq}(k)$ is shown in Fig. 2c. The diffusion of power is expected to originate from the probability distribution of periods. There was a large peak in $k_{max} = 123$ and more peaks were detected in about 250 and 380, which were multiples of 123. These were considered to be subpeaks, i.e., the second and third peaks in the diffraction. It must be noted that $P(k)$ existed in the frequency domain, while the probability distribution of periods is in the image domain. Then, the domain transformation was introduced. $P(k)$ was transformed to *Period* (τ) as already described. Subpeaks were overlapped at high frequency in the case of $P(k)$, and at low frequency in the case of *Period* (τ). If excluding this influence of subpeaks, the form of the main peak will be equivalent to the frequency distribution of distance among dots. That is, the form of the peak represents the degree of fluctuation. The peaks become high and sharp when dots are periodically arranged, whereas the disorder of the period, i.e., high fluctuation, results in a wide peak. To evaluate peak diffusion, we used the normal distribution analysis that was established mathematically, and the standard deviation σ was selected. As a result of peak separation, the main peak was separated from a secondary peak (Fig. 4c). The correlation coefficient R was poor because the higher-order (second and third) peaks were considered as one subpeak. Relative standard deviations σ_r (100 σ/Max-s) were also calculated for comparisons among materials (Table 2 and Fig. 5a,b). Figure 5a,b was reconstructed from Max-s and Fig. 5c was constructed from Max-o. We proposed σ_r as the index of an arrangement's fluctuation. When the fluctuation is evaluated and expressed as σ_r in this way, cell arrangement disorder can be compared among tree species or among organizations.

Regarding $P_{eq}(k)$ (see arrows in Fig. 2c and Fig. 4), there is a small peak on the main peak. This implies two periods along the radial direction. When the input image was observed once more, some latewood-like bands of about

30 μm in the radial direction and with a slightly thicker wall were present in *Agathis*. After such tracheids were cut off before dot mapping, the small peaks disappeared. In *Cryptomeria* sampled only from earlywood, such a small peak was not detected. There was a peak in addition to the main peak on $P_{mer}(k)$ (arrow in Fig. 2d). This peak of the frequency domain implies a shorter period between radial files. In *Cryptomeria*, a shorter period also existed. These periods were perhaps caused by a decrease in the tangential diameter of the tracheid tip part. Max-s will be examined by OAIA and the results will be described in the following report.

As for the oblique arrangement of cells, we mentioned only the most frequent direction. However, it was expected that the fluctuations in any direction could be expressed by the synthesis of both vectors because σ_r of radial and tangential directions were already detected. Future studies are needed to determine the most suitable direction for analysis.

For *Magnolia*, the period of dots was vague, and power was wide and diffusive as mentioned in the previous reports.[9,10] When we made wood fiber images of only the body and the tip was excluded, spots were clearer in the DcDM-PSP and sNM-PSP (Fig. 3d,f). However, because it was dimmer than in *Agathis* and *Cryptomeria*, the maximal part was detected but the fluctuation could not be examined. In hardwoods, wood fiber arrangement was inevitably disturbed because of the presence of vessels. E_{SPN} must be reconsidered, because there were about five periodic numbers in *Magnolia*, and the main peak was diffuse. Hardwoods have many properties that are different from those of softwoods and analysis is more difficult. However, because *Magnolia* has the most ambiguous arrangement of characteristics, we want to examine more species in greater detail.

Many cells were analyzed at a time in this report and characteristics of cell arrangements were expressed by use of the most frequent periodicity and "fluctuation." A series of techniques to reconstruct cell shapes will be completed after the direction information of the walls is examined as well as these factors in the following report. Various examinations, namely, feature extraction, feature comparison in many species, a grasp of the shape change within annual rings, and so on, can be performed using this method. The meaning of cell shape will finally be clear.

References

1. Fujita M, Midorikawa Y, Ishida Y (2002) Experimental conditions for quantitative image analysis of wood cell structure I: evaluation of various errors in ordinary accumulation image analysis (in Japanese). Mokuzai Gakkaishi 48:332–340
2. Ishida Y, Fujita M (1999) Quantitative evaluation of cell wall thickness by the Fourier transform image analysis (in Japanese). Abstracts of 49th Annual Meeting of the Japan Wood Research Society, Tokyo, p 1
3. Kino M, Ishida Y, Doi M, Fujita M (2003) Experimental conditions for quantitative image analysis of wood cell structure III: precise measurements of wall thickness (in Japanese). Mokuzai Gakkaishi 50:1–9
4. Fujita M, Kaneko T, Hata S, Saiki H, Harada H (1986) Periodical analysis of wood structure I: some trials by the optical Fourier transformation (in Japanese). Bull Kyoto Univ Forest 60:276–284
5. Fujita M, Hata H, Saiki H (1991) Periodical analysis of wood structure IV: characteristics of the power spectral pattern of wood sections and application of non-microscopic wood pictures. Mem Coll Agr Kyoto Univ 138:11–23
6. Fujita M, Saiki H, Norimoto M (1991) Anisotropic periodicity analysis on cell distribution and microfibril orientation by the various diffraction methods. Grant-in-Aid for Scientific Research (Category B) Result report from Japan Society for the Promotion of Science
7. Hata S, Fujita M, Saiki H (1989) Periodical analysis of wood structure II: dimensional arrangements of rays (in Japanese). J Soc Mater Sci Jpn 38:733–739
8. Fujita M, Ohyama M, Saiki H (1996) Characterization of vessel distribution by Fourier transform image analysis. In: Lloyd AD, Adya PS, Brian GB, Leslie JW (eds) Recent advances in wood anatomy. Forest Research Institute, New Zealand, pp 36–44
9. Maekawa T, Fujita M, Saiki H (1993) Characterization of cell arrangement by polar coordinate analysis of power spectral patterns (in Japanese). J Soc Mater Sci Jpn 42:126–131
10. Fujita M, Saiki H, Takabe K (1994) Characterization and automatic identification of woods by the Fourier transform and autocorrelation function. Grant-in-Aid for Scientific Research (Category B) Result report from Japan Society for the Promotion of Science
11. Midorikawa Y, Fujita M (2003) Experimental conditions for quantitative image analysis of wood cell structure IV: general procedures of Fourier transform image analysis (in Japanese). Mokuzai Gakkaishi 50:73–82
12. Ogata Y, Kadokawa T, Fujita M (2002) Experimental conditions for quantitative image analysis of wood cell structure II: non-microscopic image sampling over very wide areas using a film scanner (in Japanese). Mokuzai Gakkaishi 48:341–347
13. Diao X, Furuno T, Uehara T (1996) Analysis of cell arrangements in softwoods using two-dimensional fast Fourier transform (in Japanese). Mokuzai Gakkaishi 42:634–641
14. Hippo Family Club (1988) Fourier transform and uncertainty principle. In: Transnational College of LEX (ed) Who is Fourier? A Mathematical Adventure. Institute for Language Experience, Experiment & Exchange, Tokyo, pp 368–384